Surface Color Estimation Based on Inter- and Intra-Pixel Relationships in Outdoor Scenes

Shun Hirose
Nara Institute of Science and Technology
8916-5, Takayama-cho, Ikoma, Nara, Japan
shun-h@is.naist.jp

Tsuyoshi Suenaga
Nara Institute of Science and Technology
8916-5, Takayama-cho, Ikoma, Nara, Japan
tsuyo-s@is.naist.jp

Kentaro Takemura
Nara Institute of Science and Technology
8916-5, Takayama-cho, Ikoma, Nara, Japan
kenta-ta@is.naist.jp

Rei Kawakami
University of Tokyo
4-6-1, Komaba, Meguro-ku, Tokyo, Japan
rei@cvl.iis.u-tokyo.ac.jp

Jun Takamatsu
Nara Institute of Science and Technology
8916-5, Takayama-cho, Ikoma, Nara, Japan
j-taka@is.naist.jp

Tsukasa Ogasawara
Nara Institute of Science and Technology
8916-5, Takayama-cho, Ikoma, Nara, Japan
ogasawar@is.naist.jp

Abstract

We propose a method for estimating inherent surface color robustly against image noises from two registered images taken under different outdoor illuminations. We formulate the estimation based on maximum likelihood manner while considering both inter-pixel and intra-pixel relationships. We define inter-pixel relationship based on stochastic behavior of image noises and properties of outdoor illumination chromaticity. We rely on the spatial continuity of both surface color and illumination to define intra-pixel relationship. We also propose to maximize the estimation function in two step manner. Experimental results demonstrate the significant improvement of the proposed method in estimation accuracy compared to previous methods.

1. Introduction

Color is one of the most important features on computer vision algorithms, from object recognition to estimation of photometric properties. However, color information observable by camera is multiplication of both illumination and surface color, hence we must estimate illumination in the scene to infer surface color, which is invariant to illumination changes.

In general, this surface-color-estimation or *color constancy* problem is ill-posed, because it has to estimate two unknown parameters, *i.e*. surface color and illumination, from one input pixel value. Most of the related methods assume that a scene is lit by uniform illumination. But in actual situation a scene includes multiple illuminations like shadow and direct sunlight.

Unlike the aforementioned methods, Finlayson *et al*. [11] solved this ill-posed problem by using the profile of outdoor illumination, which can be linearized. Though their algorithm is sensitive to inevitable image noises, Kawakami *et al*. [22] extended Finlayson's algorithm [11] to remove the effect of the image noises in a deterministic, not probabilistic, manner.

We propose a method to robustly estimate surface color and illumination from the same input as Finlayson's method: two registered images captured under different outdoor illuminations. We use both inter-pixel (*i.e*. pixel-wise) and intra-pixel (*i.e*. spatial) relationships to make the method robust to image noise. First, we formulate inter-pixel relationship by exploiting knowledge of physics-based vision and stochastic behavior of image noises. Next, we formulate intra-pixel relationship by assuming spatial continuity in illumination as well as surface color. Then, we verify the effectiveness of considering inter- and intra-pixel relationships.

The contributions of this paper are the following:

1. We formulate color constancy problem in the probabilistic framework. As a result, image noises can be handled more simply.

978-1-4244-6983-3/10/$26.00 ©2010 IEEE

2. We propose a method for estimating plausible solution of the higher order, non-parametric Markov random field with complicated topology to solve this color constancy problem.

The rest of this paper is organized as follows: after reviewing related work in Section 2, we describe the theoretical background about color constancy and outdoor illumination in Section 3. In Section 4, we describe our surface-color-estimation method. In Section 5, we show actual implementation, such as modeling of image noises and outdoor illumination, and the optimization method which we employ. In Section 6, we show the experimental results to verify the effectiveness of the proposed method. Section 7 concludes this paper.

2. Related Work

Various methods for estimating an object's surface color have been proposed. Although several methods [24, 26, 33] rely on the Neutral-Interface-Reflection (NRI) assumption, that is, color of specular reflection assumes to be illumination color, we only deal with diffuse objects, which do not have any specular reflection. As mentioned above, most of the methods assume that a scene is lit by uniform illumination. These methods are roughly classified into two classes: one class relies on heuristics and the other class uses training data and machine learning.

In the former, the Gray-World algorithm [4] assumes that the average color in a usual scene is gray. In the same analogy, the Gray-Edge algorithm [36] assumes that the average edge difference in a scene is achromatic. The Scale-By-Max method [25] adjusts intensity range in each color channel so that the maximum intensities are the same. Gijsenij and Gevers [16] proposed to adaptively select the above color constancy algorithms depending on types of target images.

In the latter, the normalization approach, which is an extension of the Scale-By-Max method, decides the scaling factor considering the distribution of outdoor illumination [1, 14, 15]. Gamut mapping [15] maps the current gamut, *i.e.*, convex hull of color samples, to the prelearned gamut under standard illumination. Perspective color constancy applies gamut mapping in the chromaticity, not RGB, space [10]. Color-By-Correlation uses the correlation between illumination and the observed color distribution [12, 2]. Neural networks [6, 8, 5, 17, 27, 29, 35] directly learn and estimate the relationship between illumination and the color distribution. However, since these methods statistically estimate surface colors, images dissimilar from the training images are difficult to handled.

A few methods estimate multiple illuminations from an image. Ebner [9] applies the Gray-World algorithm separately to each window on the image. Hsu *et al*. [18] assumes that a scene consists of a small set of material colors. Unlike these methods, our method estimates inherent surface color and illumination in each pixel using maximum likelihood.

3. Theoretical Background

3.1. Illumination, Surface Color, and Pixel Intensity

The pixel intensity of a diffuse object is generally described as:

$$I_C = \int_\Omega S(\lambda)E(\lambda)q_C(\lambda)d\lambda, \tag{1}$$

where λ represents some spectral wavelength. I_C is the sensor response and C ($\in \{R, G, B\}$) indicates from which filter (red, green, or blue) the response is obtained. $S(\lambda)$ is the surface spectral reflectance and $E(\lambda)$ is the illumination spectral power distribution. $q_C(\lambda)$ is the three-element function of sensor sensitivity. The sensor response is calculated by integrating over the visible spectrum Ω.

Like [11], by assuming that the camera's sensitivity is very narrow, *i.e.*, regarded as the Dirac delta function, Equation (1) can be written as:

$$I_c = S_c E_c. \tag{2}$$

We define the vector (S_R, S_G, S_B) as *surface color*.

3.2. Outdoor Illumination

In this paper, we rely on the fact that outdoor illumination can be approximated by a black body radiator, which has already been proved in [20, 13]. Planckian locus is the path or locus that the color of an incandescent black body would take in a particular chromaticity space as the black body temperature changes. The spectral power distribution of its radiation, $B(\lambda)$, is formulated as Planck formula in Equation (3).

$$B(\lambda) = \frac{c_1}{\lambda^5}(e^{\frac{c_2}{\lambda kT}} - 1)^{-1}, \tag{3}$$

where $c_1 = 3.7418 \times 10^{-16}$ [Wm^2], $c_2 = 1.4388 \times 10^{-2}$ [mK], λ is wavelength [m], and T is temperature in Kelvin. By combining it with Equation (2), we can obtain a camera response under outdoor illumination:

$$I_C = aS_C B_C(T), \tag{4}$$

where a is a scaling value. Considering the inverse chromaticity space,

$$i_c = \frac{I_c}{I_B} \quad (c \in \{R, G\}), \tag{5}$$

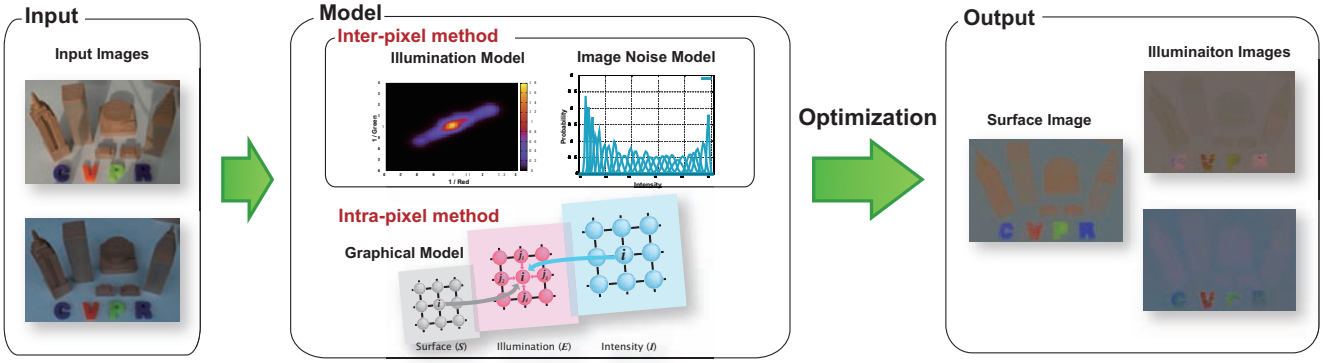

Figure 1. Overview of the proposed method. The two registered images taken under different outdoor illuminations are used as input. The method estimates surface color and illumination by considering inter-pixel and intra-pixel relationships based on the maximum likelihood manner.

which is employed in [11], the sensor response i_c in the space is formulated as:

$$i_c = s_c b_c(T), \tag{6}$$

where s_c and $b_c(T)$ are surface color and illumination in the chromaticity space.

The important point is that the outdoor illumination is parametrized by only one parameter T. We use the fact that simultaneous equation system for the estimation is solvable, since there are four unknown variables (two illumination temperatures and one two-DOF surface chromaticity) and four constraints obtained from the two registered images [23].

4. Proposed Method

4.1. Inter-Pixel Relationship

In this method, surface color is estimated from two registered images which are captured under different illuminations. Since the images have already been registered, the corresponding pixel of two images are observations of the surface lit by different illuminations. Thus, there are two inputs, I_1, I_2 and there are three unknowns, surface color S and two illumination colors E_1, E_2 in each pixel.

We estimate these unknowns by maximum likelihood estimation, since the statistical behavior of image noises, rather than noise itself, is tractable. In detail, we maximize the posterior probability of $p(S, E_1, E_2|I_1, I_2)$ for each pixel.

This probability density function can be decomposed as Equation (7) by Bayes' theorem.

$$p(S, E_1, E_2|I_1, I_2) \propto p(I_1, I_2|S, E_1, E_2)p(S, E_1, E_2). \tag{7}$$

Since we can assume the independence of all the variables, Equation (7) can be decomposed as Equation (8):

$$p(S, E_1, E_2|I_1, I_2) \propto p(I_1|S, E_1)p(E_1)p(I_2|S, E_2)p(E_2), \tag{8}$$

where $p(S)$ is assumed to be uniform distribution.

The first and third terms in the right hand of Equation (8) can be replaced with $p(I|\tilde{I}(\stackrel{\text{def}}{=} SE))$. This means multiplication of surface color and illumination corresponds to the noise-free intensity $\tilde{I}$. This likelihood represents the image noise profile, that is, the likelihood that the observed intensity is I when the noise-free intensity is $\tilde{I}$.

4.2. Intra-Pixel Relationship

In this section, we propose the estimation method robust to image noise by using intra-pixel relationship. In many cases, surface color and illumination can be smoothly changed in the image. To use this assumption of spatial continuity, we formulate the estimation as:

$$\begin{aligned} F &= p(\{S_i\}, \{E_{1i}\}, \{E_{2i}\}|\{I_{1i}\}, \{I_{2i}\}) \\ &= \prod_{i \in I} p(S_i, E_{1i}, E_{2i}|I_{1i}, I_{2i}) \prod_{j \in N(i)} p(S_i, S_j) \\ &\quad \cdot \prod_{j \in N(i)} p(E_{1i}, E_{1j}) \prod_{j \in N(i)} p(E_{2i}, E_{2j}), \end{aligned} \tag{9}$$

where i, j are positions on image coordinates, I is the set of all the pixels on the image, $N(i)$ is the set of four neighborhood pixels of i, and $p(S_i, S_j)$, etc. represent spatial dependency in either surface color or illumination space.

4.3. Maximization

Before estimating the surface color by maximizing the posterior likelihood (Equations (8) and (9)), we consider the following issues:

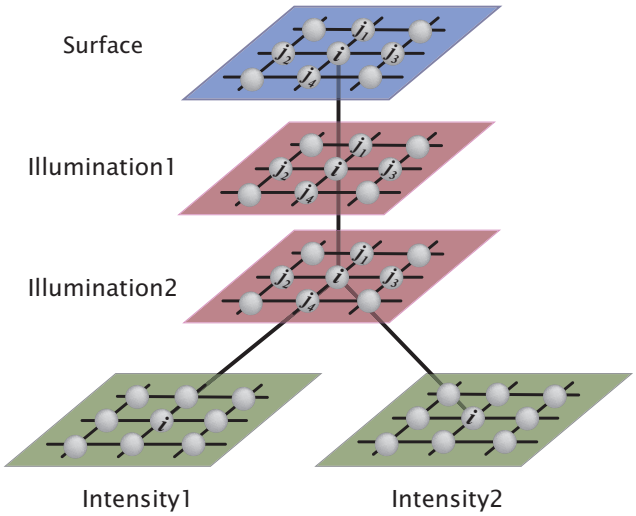

Figure 2. Graphical model of the estimation. The estimation of illumination E_{1i}, E_{2i} and surface color S_i depends on input images I_{1i}, I_{2i} and the four neighbors E_{1j}, E_{2j} and S_j.

- Which color space to use?
- Which method to use to maximize Equation (9)?

Unlike methods [11, 22], which employ the chromaticity space, we employ the RGB space, since image noises come up in the RGB space. Also, ambiguity about the scales of surface color and illumination should be considered; the following equation holds for all the real value a.

$$S'E' = (aS)(1/aE) = SE.$$

To solve this ambiguity, we assume $\sqrt{S_R^2 + S_G^2 + S_B^2} = 1$.

Maximizing Equation (9) is equal to maximizing the second order non-parametric Markov random field (MRF) (Figure 2). And the number of variables is three times larger than the number of pixels. Although to use the state-of-the-art maximization methods, such as [31, 19, 30], is one of the solutions, calculation time and memory consumption is heavy even when the size of image is moderate.

We use the Iterated Conditional Modes (ICM) method [3] to maximize Equation (9) in MRF. The weakness of the ICM method is that it is easy to get trapped at the local minima. But this weakness can be solved by giving the appropriate initial guess, which can be obtained by using Equation (8), *i.e.*, pixel-wise maximization.

5. Implementation

5.1. Modeling of Outdoor Illumination

For modeling the distribution of outdoor illumination, we took pictures of white reflectance target from sunrise to sunset. White balance function of digital camera is turned off to prevent compensation of illumination. Figure 3 shows illumination distribution in the inverse chromaticity space in Equation (5). It supports the validity of approximating illumination using one-degree line of the Planckian locus.

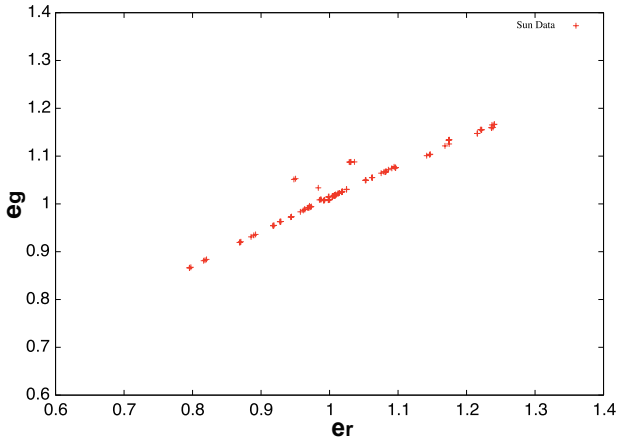

Figure 3. Illumination distribution obtained by actual measurement. The distribution limits around the line.

The probability density function of outdoor illumination is defined by non-parametric Kernel density estimation [7], as

$$\begin{aligned} p(E) &= f(e_r, e_g) \\ &= \frac{1}{Nh}\sum_{i=1}^{N} K\left(\frac{e_r - e_{ri}}{h}\right) K\left(\frac{e_g - e_{gi}}{h}\right), \\ K(x) &= \frac{1}{\sqrt{2\pi}} e^{-\frac{1}{2}x^2}, \end{aligned} \tag{10}$$

where $K(x)$ is the kernel function, N is the total number of illumination samples, and h is a smoothing parameter. In this paper, h is empirically set to 0.05. Figure 4 shows the probability density of illumination. Note that when calculating the probability density function, illumination parameters in the RGB space is converted to that in the chromaticity space.

5.2. Noise Measurement

As shown in [34, 32], noise distribution and variance depend on levels of noise-free intensity. Thus, noise distribution is estimated at each intensity value. Suppose we have a set of images of static scene taken from a fixed viewpoint with the same camera parameters as input. Fluctuation in each pixel among the images originates from image noise only. Intensity histograms are made up at each pixel from a set of images. The most frequently appearing intensity can be assumed as a noise-free intensity. Noise distribution in the entire images is constructed by merging them. Figure 5 shows noise distributions in several intensity levels. We ap-

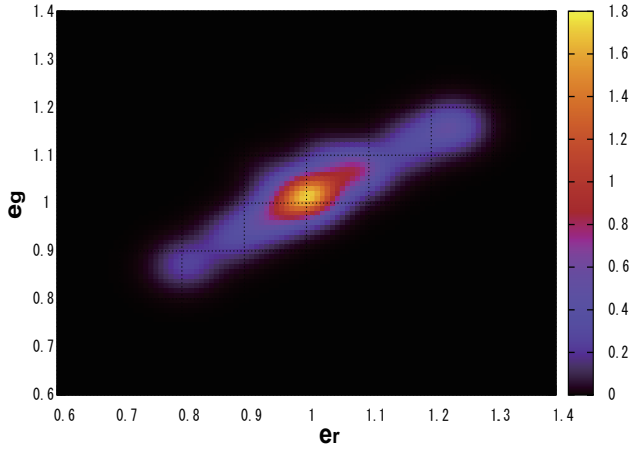

Figure 4. Probability density function of illumination.

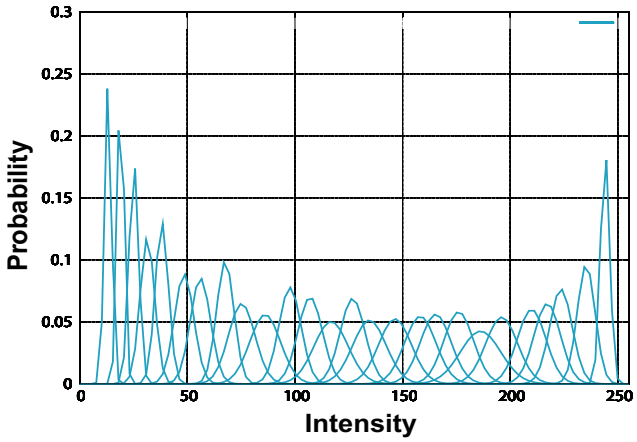

Figure 5. The noise distribution in the red channel. Noise profiles depend on their intensity levels.

proximate the noise distribution as Gaussian distribution in the estimation.

5.3. Spatial Dependency

As shown in Figure 2, we use the spatial dependency of four neighborhood pixels in surface-color and illumination images. We use Gaussian distribution to represent this dependency. Thus, the parameters of the dependency are smoothness of surface-color and illumination images.

5.4. Optimization

We sequentially optimize Equations (8) and (9). For optimization of Equation (8), we use the Down-hill simplex method [28]. Initial value of parameters are set by Finlayson's estimation, or randomly.

For optimization of Equation (9), we begin with the pixel-wise estimation, *i.e.*, Equation (8), as initial guess and use the ICM method [3]. This method maximizes the energy function by changing several (usually one) of the parameters while keeping the others fixed. This partial maximization is iterated until convergence of the function while changing the unfixed parameters.

We use the Newton method to maximize Equation (9) with one free parameter. We show the case in the maximization using E_{1i}. The other cases are dealt with in the same manner. We take the logarithm of Equation (9) and then calculate its derivative to estimate parameters of extremum. All the terms but the third and fourth terms in right hand of Equation (11) are simple quadratic forms after taking the logarithm and the derivative is easy to take. The third and fourth terms are approximated as Taylor series of $p(E_{1i})$ around E_{1i}^t, the estimation at the t-th iteration. The maximization with E_{1i}^{t+1} is done by solving Equation (9).

$$\begin{aligned}\frac{\partial \ln(F)}{\partial E_{1i}} &= \sum_{j\in N(i)} \frac{E_{1i}^{t+1} - E_{1j}^t}{\sigma_a^2} - \frac{S_i^t(I_{1i} - S_i^t E_{1i}^{t+1})}{\sigma_n^2} \\ &- \frac{P'(E_{1i}^t)}{P(E_{1i}^t)} \\ &- \frac{P''(E_{1i}^{t+1} - E_{1i}^t)P(E_{1i}^{t+1} - E_{1i}^t) - P'(E_{1i}^t)}{P(E_{1i}^{t+1} - E_{1i}^t)^2} \\ &= 0. \end{aligned} \tag{11}$$

The superscript t indicates the estimation in the t-th iteration.

6. Experiments

We conducted experiments to quantitatively evaluate the proposed method. We show the experimental results of the two proposed methods (using pixel-wise relationship only, and both pixel-wise and spatial relationships) compared to the prior methods [11, 21] using images of the Gretag Macbeth Color Checker. We also show the result of another outdoor scene.

6.1. Quantitative Evaluation

Method We used the images which include the Gretag Macbeth Color Checker and white reflectance target in this experiment. We took RAW images using DSLR camera *Nikon D60* and developed them by *Adobe Photoshop Lightroom* to uncompressed TIFF images without compensation of illumination. ISO sensitivity of the digital camera was fixed, since the noise distribution differs with ISO sensitivity.

For quantitative evaluation, we used 18 color patches of the color checker and white reflectance target. To obtain the ground truth, we set up the situation where illumination is uniformly distributed and thus illumination effect are estimated from the white reflectance target. To reduce image

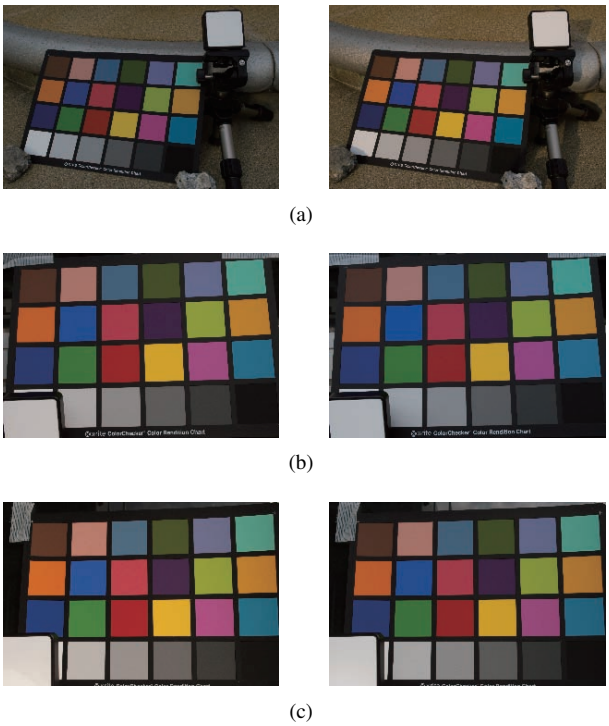

Figure 6. Input image pairs of the Macbeth Color Checker taken under different outdoor illuminations.

noise effects, the ground-truth surface color is obtained by averaging pixel values of each patches (30×30 pixels in this experiment).

We define the difference between the estimated and ground truth as the angular error in the RGB space:

$$\frac{\tilde{R}R + \tilde{G}G + \tilde{B}B}{\sqrt{R^2 + G^2 + B^2}\sqrt{\tilde{R}^2 + \tilde{G}^2 + \tilde{B}^2}}.$$

$\tilde{R}, \tilde{G}, \tilde{B}, R, G, B$ are respectively the ground truth and the estimated values in the RGB space. The angular error is usually used for the evaluation in this research area.

Result We conducted experiments using five pairs of images which were taken under different illuminations. Figure 6 are several examples of the pairs. Figure 7 shows one of the result of surface-color-estimation. From top to bottom, rows of Figure 7 show the inputs, estimation by Finlayson's [11] and Kawakami's methods [21], estimation by the proposed methods, and ground truth.

In addition, we quantitatively evaluated them by using the average estimation error. As shown in Table 1, the estimation results of our methods have better accuracy compared to the previous works [11, 21]. This result proves that it is advantageous to handle image noises by maximum likelihood manner and to handle spatial continuity by MRF framework in estimation of surface colors.

Table 1. Mean RMSE of surface-color-estimation

	Mean RMSE [deg]
Finlayson '95	19.4
Kawakami '09	11.3
Pixel-wise	8.4
Pixel-wise & spatial	5.7

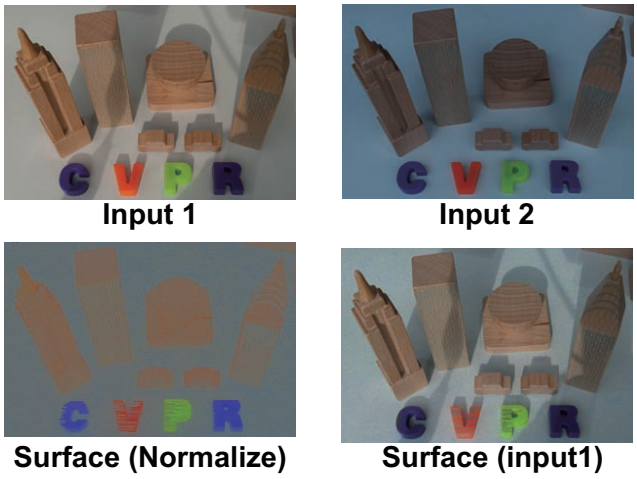

Figure 8. The result of surface-color estimation in natural scene. The top row shows input images taken at 11:00 (left) and 16:30 (right). The bottom left shows estimated surface colors. The image at the bottom right is obtained from surface color estimation at the bottom left by multiplying the brightness in input image 1.

6.2. Natural Scene

We conducted experiments with natural images, which consist of various illuminations (*i.e.*, shadow and direct sunlight). Figure 8 shows the input and the result. The top row shows input images taken at 11:00 (left) and 16:30 (right). Their illuminations vary widely. The bottom left shows the estimated surface colors. The image at the bottom right is obtained from surface color estimation at the bottom left by multiplying the brightness in input image 1. As shown in the bottom left, even if the image consists of multiple illumination, surface color is appropriately estimated.

7. Conclusion

We proposed a method for estimating object's surface color robustly against image noise from two registered images taken under different outdoor illuminations. First, we formulated surface-color-estimation based on stochastic behavior of image noise and physics-based vision in the probabilistic framework. Next, we formulated the spatial dependency of surface and illumination in the MRF framework. Then, we proposed to maximize the estimation function in two step manner.

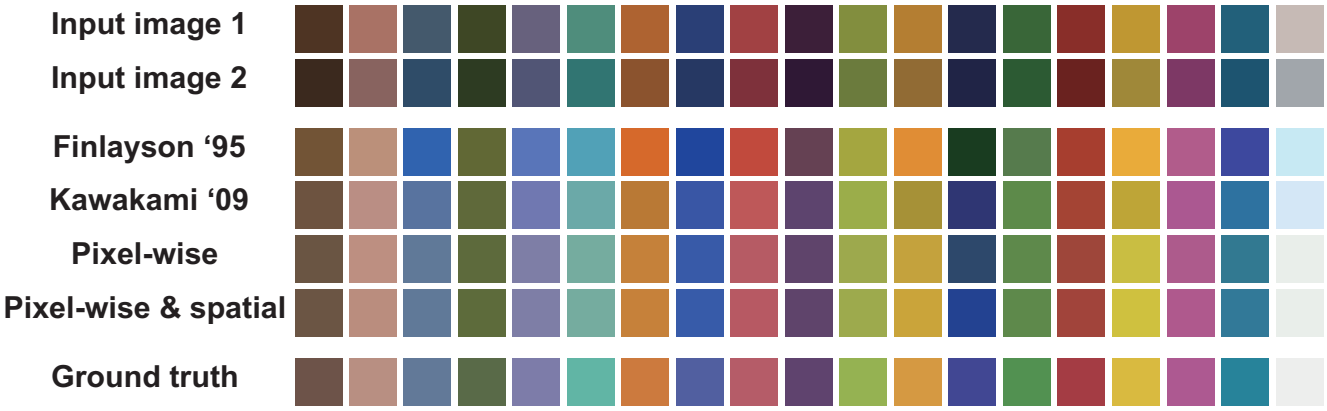

Figure 7. The result of surface-color estimation. From top to bottom, inputs, estimation by Finlayson's [11] and Kawakami's methods [21], estimation by the proposed methods, and ground truth are shown.

Our experimental results quantitatively demonstrated the effectiveness of the proposed algorithm compared to the previous methods. This result insists on the effectiveness of considering both image noise effect and spatial consistency to solve color constancy problem.

One of our future directions is to design a method to estimate only from a single image. To prepare the two registered images under different illuminations is sometimes difficult. Another direction is to estimate surface color from images which include interreflection or specular reflection. We believe that the ability to estimate illumination at each pixel is advantageous.

References

[1] K. Barnard, G. Finlayson, and B. Funt. Color constancy for scenes with varying illumination. In *Proc. of European Conf. on Comp. Vis. (ECCV)*, pages 276–287, 2004. 2

[2] K. Barnard, L. Martin, and B. Funt. Colour by correlation in a three dimensional colour space. In *Proc. of European Conf. on Comp. Vis. (ECCV)*, pages 375–389, 2000. 2

[3] J. Besag. On the statistical analysis of dirty pictures. *J. Roy. Stat. Soc. B*, 48:259–302, 1986. 4, 5

[4] G. Buchsbaum. A spatial processor model for object colour perception. *J. of The Franklin Institute 310*, pages 1–26, 1980. 2

[5] V. Cardei and B. Funt. Learning color constancy. In *Proc. of Imaging Science and Technology / Society for Information Display Fourth Color Imaging Conference*, pages 58–60, 1996. 2

[6] S. Courtney, L. Finkel, and G. Buchsbaum. A multistage neural network for color constancy and color induction. *IEEE Trans. on Neural Networks*, 6(6):972–985, 1995. 2

[7] R. Duda, D. Stork, and P. Hart. *Pattern Classification*. Wiley, John and Sons, 2000. 4

[8] P. Dufort and C. Lumsden. Color categorization and color constancy in a neural network model of v4. *Biological Cybernetics*, 65(4):293–303, 1991. 2

[9] M. Ebner. Color constancy using local color shifts. In *Proc. of European Conf. on Comp. Vis. (ECCV)*, pages 276–287, 2004. 2

[10] G. Finlayson. Color in perspective. *IEEE Trans. on Patt. Anal. and Mach. Intell.*, 18(10):1034–1038, 1996. 2

[11] G. Finlayson, B. Funt, and K. Barnard. Color constancy under varying illumination. In *Proc. of Int'l Conf. on Comp. Vis. (ICCV)*, pages 720–725, 1995. 1, 2, 3, 4, 5, 6, 7

[12] G. Finlayson, S. Hordley, and P. Hubel. Color by correlation: A simple, unifying framework for color constancy. *IEEE Trans. on Patt. Anal. and Mach. Intell.*, 23(11):1209–1221, 2001. 2

[13] G. Finlayson and G. Schaefer. Solving for colour constancy using a constrained dichromatic reflectionmodel. *Int. J. of Comp. Vis.*, 42(3):127–142, 2002. 2

[14] D. Forsyth. A novel approach to colour constancy. In *Proc. of Int'l Conf. on Comp. Vis. (ICCV)*, pages 9–18, 1988. 2

[15] D. Forsyth. A novel algorithm for color constancy. *Int. J. of Comp. Vis.*, 5(1):5–36, 1990. 2

[16] A. Gijsenij and T. Gevers. Color constancy using natural image statistics. In *Proc. of Comp. Vis. and Patt. Recog. (CVPR)*, pages 1–8, 2007. 2

[17] J. Herault. A model of colour processing in the retina of vertebrates: From photoreceptors to colour opposition and colour constancy phenomena. *Neurocomputing*, 12(2-3):113–129, 1996. 2

[18] E. Hsu, T. Mertens, S. Paris, S. Avidan, and F. Durand. Light mixture estimation for spatially varying white balance. *ACM Trans. on Graphics*, 27(3):70–70, 2008. 2

[19] M. Isard. Pampas: real-valued graphical models for computer vision. In *Proc. of Comp. Vis. and Patt. Recog. (CVPR)*, pages 613–620, 2003. 4

[20] D. Judd, D. MacAdam, and G. Wyszecki. Spectral distribution of typical daylight as a function of correlated color temperature. *J. of the Optical Society of America*, 54(8), 1964. 2

[21] R. Kawakami and K. Ikeuchi. Color estimation from a single surface color. In *Proc. of Comp. Vis. and Patt. Recog. (CVPR)*, 2009. 5, 6, 7

[22] R. Kawakami, K. Ikeuchi, and R. Tan. Consistent surface color for texturing large objects in outdoor scenes. In *Proc. of Int'l Conf. on Comp. Vis. (ICCV)*, volume 2, pages 1200–1207, 2005. 1, 4

[23] R. Kawakami, J. Takamatsu, and K. Ikeuchi. Color constancy from blackbody illumination. *J. of the Optical Society of America*, 24-7:1886–1893, 2007. 3

[24] G. J. Klinker, S. A. Shafer, and T. Kanade. The measurement of highlights in color images. *Int. J. of Comp. Vis.*, 2(1):7–26, 1992. 2

[25] E. Land and J. McCann. Lightness and retinex theory. *J. of the Optical Society of America*, 61(1):1–11, 1971. 2

[26] H. Lee. Method for computing the scene-illuminant chromaticity from specular highlights. *J. of the Optical Society of America*, 3(10):1694–1699, 1986. 2

[27] A. Moore, J. Allman, and R. Goodman. Real time neural system for color constancy. *IEEE Trans. on Neural Networks*, 2(2):237–247, 1991. 2

[28] J. Nelder and R. Mead. The downhill simplex method. *Computer Journal*, 7:308–310, 1965. 5

[29] C. Novak and S. Shafer. *Supervised color constancy for machine vision*. Jones and Bartlett Publishers, Inc., 1992. 2

[30] M. Park, Y. Liu, and R. Collins. Efficient mean shift belief propagation for vision tracking. In *Proc. of Comp. Vis. and Patt. Recog. (CVPR)*, pages 1–8, 2008. 4

[31] E. Sudderth, T. Ihler, W. Freeman, and A. Willsky. Nonparametric belief propagation. In *Proc. of Comp. Vis. and Patt. Recog. (CVPR)*, pages 605–612, 2003. 4

[32] J. Takamatsu, Y. Matsushita, and K. Ikeuchi. Estimating camera response functions using probabilistic intensity similarity. In *Proc. of European Conf. on Comp. Vis. (ECCV)*, 2008. 4

[33] R. Tan, K. Nishino, and K. Ikeuchi. Color constancy through inverse-intensity chromaticity space. *J. of the Optical Society of America*, 21(3):321–334, 2004. 2

[34] Y. Tsin, V. Ramesh, and T. Kanade. Statistical calibration of ccd imaging process. In *Proc. of Int'l Conf. on Comp. Vis. (ICCV)*, pages 480–487, 2001. 4

[35] S. Usui and S. Nakauchi. A neurocomputational model for colour constancy. In *Selected Proceedings of the International Conference*, pages 475–482, 1997. 2

[36] J. van de Weijer, T. Gevers, and A. Gijsenij. Edge-based color constancy. *IEEE Trans. on Neural Networks*, 16(9):2207–2214, 2007. 2